

Measurements of Non-volatile and volatile ($\sim 198^\circ\text{C}$) particulates were made at high altitude in the exhaust plumes of the following rockets: Atlas IIAS (AC-154 4/12/99 CCAS); Delta II (268-Landsat 7, 4/15/99 VAFB); Athena II (IKONOS, 9/24/99 VAFB); STS-106 (9/8/00, CCAS).

Size distributions and particulate concentration profiles of total and non-volatile particulates extending over the size range of 8-4000nm have been measured and will be presented. Data in the size range 340-4000nm was collected throughout the flight using laser particle counting techniques. Data in the size range 8-250nm were acquired only during plume incursions using a Grab Tank Sampling system [1].

Three modes were observed in the particulate size distributions for all launches studied. The relative mass fractions present in each mode will be discussed. A volatile component was observed for the first time in both the Athena II and STS-106 measurement flights and their mass ratios with respect to total estimated mass will be presented.

REFERENCES 1) Ross, M.N., P.D. Whitefield, D.E. Hagen and R. Hopkins, "In-Situ Measurement of the Aerosol Size Distribution in Stratospheric Solid Rocket Motor Exhaust Plumes", *Geophys. Res. Lett.* 26, 819-822. (1999).

A52B-0162 1330h POSTER

Water Vapor Enhancements in an Athena II Rocket Plume

Robert L Herman¹ (818-393-4720; robert.herman@jpl.nasa.gov)

Randall R Friedl¹ (818-354-3800; randall.r.friedl@jpl.nasa.gov)

Bruce W Gandrud² (303-497-1038; gandrud@ucar.edu)

¹Jet Propulsion Laboratory, California Institute of Technology, Mail Code 183-401 4800 Oak Grove Drive, Pasadena, CA 91109, United States

²National Center for Atmospheric Research, P.O. Box 3000, Boulder, CO 80307, United States

One of the major goals of the Atmospheric Chemistry of Combustion Emissions Near the Tropopause (ACCENT) mission was to quantify rocket plume emissions and chemistry. On September 24, 1999, the NASA WB-57F aircraft intercepted an Athena II rocket plume multiple times in the lower stratosphere. Within the rocket plume, water vapor was enhanced two to four times above the background mixing ratio of 4.6 ppmv due to oxidation of the hydroxyl-terminated polybutadiene rocket propellant. Particle concentrations were also enhanced in the rocket plume. In this talk, we will address the following questions: What is the emission index (EI) of water from an Athena II rocket? Can plume dilution be estimated? Does a significant fraction of water condense onto particles in the rocket plume?

A52B-0163 1330h POSTER

Mass-Independent Fractionation of Oxygen-containing Radicals in the Atmosphere

James R Lyons (310-794-5047; jrl@ess.ucla.edu)

UCLA, Department of Earth and Space Sciences, Los Angeles, CA 90095-1567, United States

Mass-independent fractionation (MIF) of ozone has been observed in both the troposphere and stratosphere (e.g., Thiemens, 1999). Because ozone is a photochemically active species, its MIF signature can be imparted to other atmospheric molecules. Using a photochemical equilibrium model for short-lived radical species, I have computed the expected MIF for typical mid-latitude conditions. The model accounts for about 70% of recent measurements of $\Delta^{17}\text{O}$ for H_2O_2 in rainwater (Savarino et al., 1999), and predicts large MIF for NO_x and ClO species ($\sim 40\text{--}70\text{‰}$), and their products (ClONO_2 and HNO_3). Furthermore, in the stratosphere oxygen exchange reactions between OH and NO_x yield OH with $\Delta^{17}\text{O}$ from 2 to 45 ‰. Stratospheric water produced during H abstraction by OH would be similarly mass-independently fractionated. In the troposphere rapid exchange between OH and H_2O erases any MIF signature in OH. These model results depend on several O exchange reactions with unknown activation energies or rate coefficients known only as upper limits.

The model predicts that stratospheric H_2O should have a MIF signature, thus providing an additional method for distinguishing tropospheric water transported upward (or horizontally from the tropics) from water produced chemically in the stratosphere. An upper limit to $\Delta^{17}\text{O}$ of stratospheric H_2O can be obtained from consideration of the quasi-conserved quantity $2[\text{CH}_4] + [\text{H}_2\text{O}]$ for air parcels entering the stratosphere. Dessler et al. (1994) determined that $2[\text{CH}_4] + [\text{H}_2\text{O}]$ constitutes 45 ‰ of the quasi-conserved sum, suggesting that $\Delta^{17}\text{O}$ of H_2O has an upper limit value of $\sim 20\text{‰}$. However, this value neglects return of unoxidized

CH_4 to the troposphere. One-dimensional calculations that properly account for mixing are in progress.

A52C MC: 123 Friday 1330h Sampling Issues in Observing the Atmosphere II

Presiding: I Astin, University of Reading; L Di Girolamo, University of Illinois at Urbana-Champaign

A52C-01 1330h

Cloud Cover From Linear Transect Measurements: Sampling Issues

Larry Di Girolamo¹ (217-333-3080; larry@atmos.uiuc.edu)

Ivan Astin² (011-44-1189-318741; iva@mail.nerc-essc.ac.uk)

¹University of Illinois at Urbana-Champaign, Department of Atmospheric Sciences 105 S. Gregory Street, Urbana, IL 61801 3070, United States

²University of Reading, NERC Environmental System Science Center, Reading, United Kingdom

Space-based cloud radars and lidars provide linear transect measurements along their orbital path. Their measurements are divided into smaller finite linear transects for analysis. A finite linear transect measurement may be assumed to be a representative sample of a geographically larger field. This assumption invites new statistical tools to be developed to tackle the sampling issues that arise. We will present two such statistical tools for examining cloud cover. The first provides the general probability distribution for the fraction of clouds along a finite transect. This distribution allows confidence intervals to be placed on the observed cloud fraction prior to measurement based on knowledge of the distributions for the cloud and clear-sky lengths. In this form, hypothesis testing of models for these length distributions can be made, given the observed cloud fraction. The second tool is derived by applying Bayes' theorem to the above distribution so that confidence intervals can be placed on the true cloud fraction. This second tool is applied to cumulus cloud fields, revealing that confidence for the true cloud fraction over typical climate model grid scales as measured by a radar or lidar in space is rather low. Finally, this approach gives a way of estimating the probability mass function for the number of clouds layers within a column perpendicular to the transect and hence the probability of a cloud layer obscuring one below.

A52C-02 1347h

Sampling Error Characteristics Of Cloud Observations From LiDAR

Martine van de Poll (44 118 935 26 99; hmvp@mail.nerc-essc.ac.uk)

NERC-ESSC, Harry Pitt Building, 3 Earley Gate, University of Reading, Reading, Ber RG6 6AL, United Kingdom

Height profiles of cloud fraction is an important parameter that is not well represented in GCMs and in smaller scale models. Improvements should come from new and existing remote sensing technologies that will increasingly provide the science community with direct observations of such profiles. However, an inherent error or uncertainty is associated with any cloud fraction estimate from remote sensing data due to instrument and atmospheric noise, sensor resolution and the sampling scheme. While all sources of uncertainties need to be investigated further, this project focuses on the characteristics of the errors originating from the sampling scheme.

Space-borne LiDAR data from the 1994 NASA LITE campaign is used to study and quantify the characteristics of such sampling errors in cloud fraction estimates from along transect measurements. This is done within a general model for sampling along a transect, which has been developed based on an approach from queuing theory, without making prior assumptions on the type of cloud distribution (Astin and Di Girolamo, 1999).

Results will be presented giving estimates of the cloud fraction and its distributions over a range of altitudes as evaluated from cloudy and clear interval lengths as observed along the transects of the LITE observations. The estimates themselves are refined to account for missing data due to attenuation of the LiDAR signal by dense cloud.

Further, the distribution of cloud cover fraction over the earth is also presented, which allows for climatological interpretation of the results. In this, estimates of the mean cloud cover fraction and distributions and confidence intervals are provided for pressure

levels from the boundary layer to the tropopause. Estimates are also inferred from transects over the whole globe, but separated into climatological regions based on mean precipitation-evapotranspiration, as well as separated by surface type such as clouds over land versus those above sea.

The above results allow examination of the error characteristics of the cover fraction estimates in relation with the underlying process and the LiDAR sampling scheme.

A52C-03 1404h

Spatial Variability of Derived Properties for Marine Stratus Clouds

Mark Matheson¹ (541-737-5692; mmatheso@oce.orst.edu)

James A Coakley¹ (541-737-5686; coakley@oce.orst.edu)

¹Oregon State University, College of Oceanic and Atmospheric Sciences, Ocean Admin 104, Corvallis, OR 97331-5503

Cloud visible optical depth, droplet effective radius, and emission temperature retrieved from satellite imagers are validated by comparing them to the properties retrieved from ground-based remote sensing instruments or in-situ aircraft observations. This involves comparing an instantaneous two-dimensional satellite data set to a temporally averaged data set collected at one location (the ground station record) or to a linear transect (the aircraft record). To characterize some of the errors that may occur in such a comparison, cloud properties of a square region are derived from NOAA-14 1-km resolution AVHRR data. These properties are compared to a central transect of the same satellite data, which is used to simulate the cloud advecting over a ground station or an aircraft transect.

Autocorrelation lengths of all three derived cloud properties for marine stratus are less than 10 km and the autocorrelation functions fall below zero at approximately 20 km. Autocorrelations remain below zero for lags greater than 20 km probably because of mesoscale structure in the stratus fields. Such short autocorrelation lengths would appear to impose severe limits on the distances over which two cloud samples may be compared. Nevertheless, when the cloud properties averaged for the square regions are compared with the cloud properties averaged for the central transect, the area averaged and transect averaged properties are well correlated (greater than 0.975). For scales of order 30 km, the mean difference between the area averages and the transect averages is much smaller than the standard deviations of the data in an individual area, which is in turn much smaller than the range of the averages of all the areas used for analysis. This result is independent of sensor resolution for resolutions smaller than 8 km. These results indicate that cloud properties averaged for square regions can be meaningfully compared to cloud properties averaged for their central transect, supporting the use of ground instruments and aircraft transects to validate satellite retrievals.

In order to test for biases in derived cloud properties due to differences in satellite sensor and surface instrument resolution, the average cloud properties of small regions are calculated by two different methods. In the first method, radiances from each individual pixel are used to derive cloud properties, and the cloud properties are averaged over the entire area. In the second method, the radiances for the entire area are averaged and these averaged radiances are used to derive cloud properties. Of the derived cloud properties, only visible optical depth retrievals show bias, which increases with decreasing resolution. Visible optical depths calculated using the first method (derived then averaged) are lower than visible optical depths calculated using the second method (averaged then derived).

A52C-04 1421h

Analysis of Temporal Sampling Errors in CERES Data Products

Jesse D Kenyon¹ (757 827-4641; j.d.kenyon@larc.nasa.gov)

David R Doelling¹ (757 827-4634; d.r.doelling@larc.nasa.gov)

David F Young² (757 864-5740; d.f.young@larc.nasa.gov)

Takmeng Wong² (757 864-5607; TAKMENG.WONG@LaRC.NASA.GOV)

¹Analytical Services and Materials, Inc, 1 Enterprise Parkway Suite 300, Hampton, VA 23666, United States

²NASA Langley Research Center, Mail Stop 420, Hampton, VA 23681-2199, United States

The Clouds and the Earths Radiant Energy System (CERES) Experiment is the latest and most accurate satellite-based instrument designed to measure the Earths global energy budget. With improvements in instrument calibration accuracy and stability, coupled with the development of new angular directional

models, temporal sampling is the largest remaining error source for CERES regional mean fluxes. To improve sampling of the diurnal cycle, CERES was designed as a 3-satellite constellation with instruments aboard the sun-synchronous Terra and Aqua satellites and the temporally precessing TRMM spacecraft. However, the failure of the TRMM instrument in April 2000, and launch delays for Terra and Aqua resulted in single-satellite coverage for most of the mission to date. Pre-launch error analysis using two months of data from a single GOES satellite demonstrated that monthly zonal mean shortwave flux errors due to temporal sampling could exceed 10 Wm² for Terra for data processed in the manner of the ERBE experiment.

The new CERES data processing system was designed to reduce temporal sampling errors by using geostationary data to improve the interpolation of fluxes between the times of CERES observation. Pre-launch studies demonstrated that this new technique reduces instantaneous interpolation errors by over 50% for both longwave and shortwave fluxes relative to the ERBE processing. However, a final error analysis of the monthly mean fluxes that includes possible error sources from the geostationary data was not completed.

This paper will focus on a new analysis of the temporal sampling error budget for CERES. The pre-launch study has been expanded to include a twelve months of ISCCP DX data covering all longitudes. New estimates of the global and seasonal error budget will be presented for the sampling patterns of each of the CERES satellites. Results suggest that the global sampling errors may have been overestimated by using only Western Hemispheric data during convectively active months. In addition, an expanded error analysis of monthly mean fluxes will be presented that includes errors in the calibration and narrowband-to-broadband conversion of the geostationary data used in the new CERES temporal interpolation algorithm.

A52C-05 1438h

The Spatial Coherency of Spectrally Resolved Radiative Fluxes

William O'Hirok¹ (805 893 7355; bill@icess.ucsb.edu)

Catherine Gautier¹ (805 893 8095; gautier@icess.ucsb.edu)

¹Institute for Computational Earth System Science, University of California, Santa Barbara, CA 93106, United States

Properly sampling fluxes produced by the interaction of solar radiation with cloud fields is a difficult endeavor since observations can experience large deviations from the mean over short spatial and temporal scales. For understanding cloud radiative processes, it is often assumed that the relationship between spectrally resolved observations is spatially coherent and observations can be understood using plane-parallel radiative transfer models. The validity of such an approach is rarely tested. In this study, we use a 3-D radiative transfer model to understand the impact of this assumption on two different observing techniques. The first approach relates observations in the oxygen A band with broadband atmospheric absorption of solar radiation in a cloudy atmosphere. The second uses non-absorbing wavelengths to remove the effects of horizontal flux divergence in aircraft observations of inferred broadband atmospheric absorption.

A52C-06 1515h

Cloud amount retrieval for a cloud radar.

Ivan Astin¹ (iva@mail.nerc-essc.ac.uk)

Larry Di Girolamo² (larry@atmos.uiuc.edu)

¹NERC-ESSC, University of Reading, Reading RG6 6AL, United Kingdom

²Department of Atmospheric Sciences, University of Illinois at Urbana-Champaign, Urbana, IL 61801, United States

In order to detect weakly reflecting cloud layers, it is often necessary to integrate a large number of radar pulses. The number of pulses integrated (or integration time) is usually chosen so that radar returns from a cloud layer having a specified (low) pulse to pulse reflectivity will be detected. Whilst it is true that the greater the number of integrated pulses the lower is the detectable cloud reflectivity, it is not true, as is often stated, that if 90% of all clouds have a certain (pulse to pulse or integrated) reflectivity, then 90% of all clouds can be detected. This is because cloud layers tend to have variable reflectivity over the integration time. The actual amount of detectable clouds cannot be evaluated based solely on the radar sensitivity.

We will demonstrate that the amount of clouds detected depends on the radar sensitivity and the spatial or temporal distribution of the clouds, for a fixed cloud detection threshold. Thus, we will show that designing a radar with an extreme sensitivity is not sufficient, or indeed necessary, for accurate cloud amount measurements. In fact, a very high radar sensitivity will

almost always result in a large bias in measured cloud amount, if the threshold is set to the maximum sensitivity of the radar, which is the usual case. Instead, a threshold placed at a moderate reflectivity or placed at the maximum sensitivity of a moderately sensitive radar is needed for unbiased estimates of cloud amount. We will demonstrate analytically the optimum detection threshold of a radar observing the difficult to detect thin (< 200 m) liquid water clouds, whose very low reflectivity approximates a Weibull distribution. Our approach is also used to investigate the magnitude of possible biases in cloud amount for several published design concepts for both the proposed ESA space-borne cloud radar and NASA's CloudSat for a range of cloud sizes and spatial distributions.

A52C-07 1532h

Sampling errors for a nadir viewing instrument on the International Space Station

Howard I. Berger¹ (howardb@ssc.wisc.edu)

Robert Pincus² (robert@cdc.noaa.gov)

Frank Evans³ (evans@nit.colorado.edu)

Dave Santek¹ (santek@ssc.wisc.edu)

Steve Ackerman^{1,3} (SteveA@ssc.wisc.edu)

¹Space Science and Engineering Center, University of Wisconsin 1225 W. Dayton St., Madison, WI 53706, United States

²NOAA-CIRES Climate Diagnostics Center, 325 Broadway, R/CDC1, Boulder, CO 80305, United States

³Program in Atmospheric and Oceanic Sciences, 311 UCB University of Colorado, Boulder, CO 80309, United States

In an effort to improve the observational characterization of ice clouds in the earth's atmosphere, we are developing a sub-millimeter wavelength radiometer which we propose to fly on the International Space Station for two years. Our goal is to accurately measure the ice water path and mass-weighted particle size at the finest possible temporal and spatial resolution. The ISS orbit precesses, sampling through the diurnal cycle every 16 days, but technological constraints limit our instrument to a single pixel viewed near nadir.

We discuss sampling errors associated with this instrument/platform configuration. We use as "truth" the ISCCP dataset of pixel-level cloud optical retrievals, which acts as a proxy for ice water path; this dataset is sampled according to the orbital characteristics of the space station, and the statistics computed from the sub-sampled population are compared with those from the full dataset. We explore the tradeoffs in average sampling error as a function of the averaging time and spatial scale, and explore the possibility of resolving the diurnal cycle.

A52C-08 1549h

Science-Optimized Orbit Selection for the Canadian Atmospheric Chemistry Experiment (ACE)

Victor A. Wehrle¹ (1-613-991-9877; victor.wehrle@space.gc.ca)

Andrew Fratpietro¹ (1-613-991-9877)

Martin Lacelle¹ (1-613-991-9877)

¹Canadian Space Agency, 100 Sussex Drive, Ottawa, ON K1A 0R6, Canada

ACE is a solar occultation space science mission, implemented via the CSAs SCISAT-1 project. The satellite carries two instruments with a common sun-tracker and input optics: a Fourier transform spectrometer (2.4-13.3 microns) with two imagers (at 0.525 and 1.02 microns), and a dual diffraction grating spectrometer (0.285-0.55 and 0.525-1.03 microns). The satellite mass is 151 kg, power is 164 W (78 W orbit average), volume is one-half of Pegasus-XL envelope, and pointing is 3-axis stabilized within 1 deg of sun centre. The sun-tracker provides fine pointing control to the radiometric centre of the sun at an accuracy of 0.1 mrad within 1/3 of a second from a 2.5 deg offset, and achieves a stability of 0.0075 mrad RMS in the steady state. The nominal orbit is circular at 650 km/74 deg, the scheduled launch date is 21 December 2002, and the design mission lifetime is 2 years.

The overarching goal of the ACE mission, defined by Mission Scientist Peter Bernath of the University of Waterloo in terms of nine specific goals grouped into 3 levels of priority, is to measure and to understand the chemical and dynamical processes that control the distribution of ozone in the upper troposphere and stratosphere. The selection of the best orbit, i.e. whose occultation tangent point (otp) trajectory maximizes the probability of achieving this overarching goal, is not intuitively obvious.

In this paper, we employ a systematic method for selecting the science-optimized orbit for the ACE mission. We draw upon historical flight (TOMS, TOVS) and other data to define an ideal (but impossible) orbit whose latitude vs time-of-year otp trajectory yields measurements consistent with the science goals of the mission. We constrain the candidate (i.e. possible) orbits to those which yield annual repeats of their otp trajectories. From among these, we employ a Science Goodness algorithm which gives a measure of the departure of candidate trajectories from the ideal one, accounting also for the amount of lat/long motion, or geographic smear, of the otp during any given occultation event. A surprising result is that the highest rating candidate orbit is not robust in the sense that launch vehicle orbit insertion errors or unexpectedly large satellite drag could render this apparently best orbit a science mission disaster.

A52C-09 1606h

An Assessment of the Ability of Potential Satellite Instruments to Resolve Spatial and Temporal Variability of Atmospheric Carbon Dioxide

Arlyn E Andrews¹ (301-614-5856; andrews@code916.gsfc.nasa.gov)

S Randolph Kawa¹ (301-614-6004; kawa@code916.gsfc.nasa.gov)

¹NASA Goddard Space Flight Center, Mailstop 916.0, Greenbelt, MD 20771, United States

Mounting concern regarding the possibility that increasing carbon dioxide concentrations will initiate climate change has stimulated interest in the feasibility of measuring CO₂ mixing ratios from satellites. Currently, the most comprehensive set of atmospheric CO₂ data is from the NOAA CMDL cooperative air sampling network, consisting of more than 40 sites where flasks of air are collected approximately weekly. Sporadic observations in the troposphere and stratosphere from airborne in situ and flask samplers are also available. Although the surface network is extensive, there is a dearth of data in the Southern Hemisphere and most of the stations were intentionally placed in remote areas, far from major sources. Sufficiently precise satellite observations with adequate spatial and temporal resolution would substantially increase our knowledge of the atmospheric CO₂ distribution and would undoubtedly lead to improved understanding of the global carbon budget. We use a 3-D chemical transport model to investigate the ability of potential satellite instruments with a variety of orbits, horizontal resolution and vertical weighting functions to capture the variation in the modeled CO₂ fields. The model is driven by analyzed winds from the Goddard Data Assimilation Office. Simulated CO₂ fields are compared with existing surface and aircraft data, and the effects of the model convection scheme and representation of the planetary boundary layer are considered.

A52C-10 1623h

IMPLICATIONS OF NON-SYSTEMATIC OBSERVATIONS FOR VERIFICATION OF FORECASTS OF AVIATION WEATHER VARIABLES

Barbara G Brown¹ (303-497-8468; bgb@ucar.edu)

Greg S Young¹ (303-497-2809; young@rap.ucar.edu)

Tressa L Fowler¹ (303-497-8373; tressa@rap.ucar.edu)

¹National Center for Atmospheric Research, P.O. Box 3000, Boulder, CO 80307-3000, United States

Over the last several years, efforts have been undertaken to develop improved automated forecasts of weather phenomena that have large impacts on aviation, including turbulence and in-flight icing conditions. Verification of these forecasts - which has played a major role in their development - is difficult due to the nature of the limited observations available for these evaluations; in particular, voice reports by pilots (PIREPs). These reports, which are provided inconsistently by pilots, currently are the best observations of turbulence and in-flight icing conditions available. However, their sampling characteristics make PIREPs a difficult dataset to use for these evaluations. In particular, PIREPs have temporal and spatial biases (e.g., they are more frequent during daylight hours, and they occur most frequently along flight routes and in the vicinity of major airports, where aircraft are concentrated), and they are subjective. Most importantly, the observations are non-systematic. That is, observations are not consistently reported at the same location and time. This characteristic of the reports has numerous implications for the verification of forecasts

of these phenomena. In particular, it is inappropriate to estimate certain common verification statistics that normally are of interest in forecast evaluations. For example, estimates of the false alarm ratio and critical success index are incorrect, due to the unrepresentativeness of the observations. Analytical explanations for this result have been developed, and the magnitudes of the errors associated with estimating these statistics have been estimated through Monte Carlo simulations. In addition, several approaches have been developed to compensate for these characteristics of PIREPs in verification studies, including methods for estimating confidence intervals for the verification statistics, which take into account their sampling variability. These approaches also have implications for verification of forecasts of other types of phenomena where the observations are non-systematic, such as severe weather.

A52C-11 1640h

Sampling-Related Variability in Raingage Network Products

Edward I Tollerud (303-497-6127;
tollerud@fsl.noaa.gov)

NOAA Research-Forecast Systems Laboratory, 325
Broadway, Boulder, CO 80305, United States

The representation of precipitation using sparse gage measurements presents formidable challenges due to incomplete and nonhomogeneous sampling. With feasible density and frequency of observations, gage networks cannot capture the full spectrum of space and time scales at which precipitation may fall. If unrecognized or unadjusted, this sampling inadequacy can lead to a biased or distorted characterization of precipitation.

We examine the magnitude of this sampling effect on two products: gridded fields of precipitation analyzed from point observations, and verification scores for model-generated precipitation computed using these observed fields. To do so, we first directly compare analyses and frequency statistics produced using several independent U.S. raingage datasets, including measurements made by the operational array of near-real-time daily and hourly reporting rain gages acquired from the National Centers for Environmental Prediction, and two sets of high-quality raingage measurements made by volunteer observers and archived at the National Climatic Data Center. Next, to assess intra-network sampling differences, we employ resampling techniques (including bootstrapping) to estimate the variability of gridpoint precipitation values and model verification scores that must be assumed when the analyses or scores are used. We also discuss the implications of combining precipitation observations from platforms with vastly different sampling characteristics (e.g., radar and gages).

A52D MC: 133 Friday 1330h

Tropospheric Chemistry and Constituents III

Presiding: L Avallone, Laboratory for
Atmospheric and Space Physics; R
Anderson, Centre for Atmospheric
Chemistry

A52D-01 1330h

Measurements of Active Chlorine in the High Latitude Boundary Layer During Springtime

Linnea M Avallone (3034925913;
avallone@lasp.colorado.edu)

Laboratory for Atmospheric and Space Physics, Uni-
versity of Colorado 590 UCB, Boulder, CO 80309-
0590, United States

Studies of the sudden boundary-layer ozone loss phenomenon in the springtime high latitudes have concluded that catalytic reactions involving bromine species are the dominant ozone destroyers. However, calculations show that even small amounts of active chlorine and iodine can make significant contributions to the ozone loss rates during these events. In this presentation, I will describe the first in situ measurements of the halogen radical chlorine oxide (ClO) in the high-latitude boundary layer. These observations were made as part of ARCTOC '96 in Ny Alesund, Spitsbergen and Alert 2000 Polar Sunrise Experiment at Alert, Nunavut, Canada during low ozone events in the months of April and May. I will compare these observations to estimates of active chlorine abundances derived from a chemical amplification technique (Perner et al., 1999) and to published model calculations. Finally, I will explore the extent to which the observed ClO can contribute to ozone loss rates under typical high Arctic conditions.

A52D-02 1345h

Isotopic and Chemical Characterization of Particulate Nitrogen in Marine Air at Bermuda during Spring

Vaughan Turekian¹ (202-334-2547;
vturekia@nas.edu)

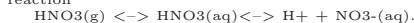
Stephan Macko² (804-982-2967; sam8f@virginia.edu)

William Keene² (wck@virginia.edu)

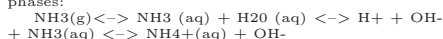
¹The National Academy of Sciences, 2100 C St NW,
Washington, DC 20418, United States

²The University of Virginia, Department of Envi-
ronmental Sciences Clark Hall, Charlottesville, VA
22903, United States

Size resolved particulate nitrogen species were measured on Bermuda during spring, 1998. NO₃⁻ was primarily associated with super-m radius aerosol and NH₄⁺ with sub-m radius aerosol, which is consistent with thermodynamic properties of the gaseous precursors and the size distribution of aerosol acidity. The average d15N for the super-m aerosol (-2.1 ± 0.5‰) was depleted in 15N relative to submicron aerosol (d15N = 5.3 ± 1.5 ‰). The d15N range between super-μm and sub-m aerosol is consistent with the different sources for NO₃⁻ and NH₄⁺. The d15N values indicate that high temperature combustion was the dominant source for the NO₃⁻. The strong correlation between the d15N for paired aerosols with geometric mean radii (GMR) 5.4 and 2.3 μm suggests that incorporation of NO₃⁻ into the aerosol was unidirectional following the reaction



There was no significant correlation between the d15N values for paired aerosols with GMR 0.34 and 0.18 μm, suggesting that NH₃ actively recycles between phases:



The dry deposition of super-m aerosol accounted for over 99

A52D-03 1400h

In Situ Measurements of Halocarbons and Greenhouse Gases from the Trans-Siberian Railway During Summer 2001

Dale F Hurst^{1,2} (303-497-7003;

Dale.Hurst@noaa.gov); Pavel A Romashkin^{1,2},
James W Elkins¹; Eva A Oberlander³; Nikolai F
Elansky⁴; Igor B Belikov⁴; Igor G Granberg⁴;
George S Gollitsyn⁴; Carl A.M. Brenninkmeijer³;
Paul J Crutzen³

¹NOAA Climate Monitoring and Diagnostics Labora-
tory, 325 Broadway R/CMDL1, Boulder, CO 80305,
United States

²CIRES, University of Colorado, Campus Box 216,
Boulder, CO 80309, United States

³Max Planck Institute for Chemistry, Dept. of Air
Chemistry, Postfach 3060, Mainz D-55020, Ger-
many

⁴Institute of Atmospheric Physics, Russian Academy
of Sciences, Pyzevsky per., 3, Moscow 109017, Rus-
sian Federation

During June 27 July 10, 2001, over 11,000 in situ measurements of CFC-12, halon-1211, N₂O, SF₆, and 5000 measurements of CFC-11, CFC-113, CHCl₃, CH₃CCl₃, CCl₄, CH₄ and H₂ were made along 17,000 km of the trans-Siberian railway between Moscow and Khabarovsk, Russia. Also measured by in situ analyzers were CO, CO₂, O₃, NO_x, and standard meteorological parameters. These measurements were part of the seventh Trans-Siberian Observations in the Chemistry of the Atmosphere (TROICA-7) scientific expedition, a collaboration between U.S., Russian, and German scientists.

Most of these gases were detected at elevated concentrations along some sections of the fully-electrified railway, typically in proximity to the larger cities. Specifically, spikes of CFC-12, halon-1211, CHCl₃ and CH₄ were frequently encountered during both the eastward and westward transects of the expedition. Attempts to identify the sources of these emissions are based on analyses of their correlations with the other measured gases. Chloroform emissions are generally uncorrelated with anthropogenic tracers, and are believed to be associated with the bleaching of wood pulp from Siberian forests. CFC-12 and halon-1211 emissions are mostly uncorrelated with one another, and accurate identification of their sources is difficult but extremely important in view of the Montreal Protocol. CH₄ emissions were detected as short-term spikes and, in some regions, broader increases in the background CH₄ concentration. Possible sources for CH₄ emissions include biomass burning, leaks from natural gas transmission lines, and wetlands.

A52D-04 1415h

Nonmethane Hydrocarbons and Ozone in the Rural Southeast United States National Parks: A Model Sensitivity Analysis and Its Comparison with Measurement

Daiwen Kang¹ ((919) 512 1405;
dkang2@unity.ncsu.edu)

Viney P. Aneja¹ ((919) 515 7808;
viney_aneja@ncsu.edu)

Rohit Mathur² (mathur@ncsc.org)

John D. Ray³ (John_D_Ray@nps.gov)

¹Department of Marine, Earth, and Atmospheric Sci-
ences, Environmental Technology Program, North
Carolina State University, Campus Box 8208,
Raleigh, NC 27695

²Environmental Programs, MCNC-North Carolina, Su-
percomputing Program, Research Triangle Park,
NC

³Air Resources Division, National Park Service, Den-
ver, Colorado

A comprehensive modeling analysis is conducted using the Multiscale Air Quality Simulation Platform (MAQSP) focusing on nonmethane hydrocarbons and ozone in three southeast United States national parks for a 15-day time period (July 14th to July 29th, 1995) characterized by high O₃ surface concentrations. Nine emission scenarios including the base scenario are analyzed. Model predictions are compared with and contrasted against observed data at the three locations for the same time period. Model predictions (base scenario) tend to give lower daily maximum O₃ concentrations than observation by 10.8% at Cove Mountain, Great Smokey Mountains National Park (GRSM), 26.8% at Mammoth Cave National Park (MACA), and 17.6% at Big Meadows, Shenandoah National Park (SHEN). Overall mean ozone concentrations are very similar at GRSM and SHEN (observed data at MACA are not available). Model predicted concentrations of lumped paraffin compounds match the observed values on the same order, while the observed concentrations for other species (isoprene, ethene, surrogate olefin, surrogate toluene, and surrogate xylene) are usually an order of magnitude higher than the predictions. Sensitivity analyses indicate each location has its own characteristics in terms of the capacity of volatile organic compounds (VOCs) to produce O₃, but a maximum VOC capacity point (MVCP) exists at all locations that changes the influence of VOCs on O₃ from production to destruction. Analysis of individual model process budgets shows that more than 50% of daytime O₃ concentrations at these rural locations are transported from other areas, local chemistry is the second largest contributor (13% to 42%), all other processes combined contribute less than 10% of the daytime O₃ concentrations. Local emissions (>99%) are predominantly responsible for VOCs at all locations, while vertical diffusion (>70%) is the predominant process to move VOCs away from the modeling grid. Dry deposition (~10%) and chemistry (2 to 13%) processes are also responsible for the removal of VOCs. Metrics such as O₃ production efficiency of VOC emissions (VOPE), VOC potential for O₃ production (VPOP), and MVCP are devised to quantitatively measure the different characteristics of O₃ production and VOCs in these rural environments. Implications of this model exercise in understanding O₃ production in rural atmospheres are analyzed and discussed. Even though this study is focusing on three United States National Parks, the research results and conclusions may be applicable to other rural atmospheres.

A52D-05 1430h

Seasonal VOC measurements at a rural site in the Sierra Nevada Mountains, California: A focus on acetone and methanol

Gunnar W Schade¹ (510-643-6449;
gws@nature.berkeley.edu)

Allen H Goldstein¹ (510-643-2451;
ahg@nature.berkeley.edu)

¹University of California Berkeley Department of
Environmental Science, Policy, and Management
Ecosystem Sciences Division, 151 Hilgard Hall,
Berkeley, CA 94720-3110

Methanol and acetone significantly influence the odd hydrogen budget of the upper troposphere. We have measured the seasonal cycle of these oxygenated volatile organic compounds (VOCs) and several other biogenic and anthropogenic VOCs along with carbon monoxide (CO) at Blodgett Forest Research Station, elevation 1300 m, on the western slope of the Sierra